Received: 14 March 2018 | Revised: 3 August 2018 | Accepted: 6 August 2018

DOI: 10.1111/ina.12499

ORIGINAL ARTICLE

WILEY

Three-dimensional printing with nano-enabled filaments releases polymer particles containing carbon nanotubes into air

Aleksandr B. Stefaniak[1] | Lauren N. Bowers[1] | Alycia K. Knepp[1] | M. Abbas Virji[1] | Eileen M. Birch[2] | Jason E. Ham[1] | J. R. Wells[1] | Chaolong Qi[2] | Diane Schwegler-Berry[1] | Sherri Friend[1] | Alyson R. Johnson[1] | Stephen B. Martin Jr[1] | Yong Qian[1] | Ryan F. LeBouf[1] | Quinn Birch[3] | Duane Hammond[2]

[1]National Institute for Occupational Safety and Health, Morgantown, West Virginia

[2]National Institute for Occupational Safety and Health, Cincinnati, Ohio

[3]Department of Chemical and Environmental Engineering, College of Engineering and Applied Science, University of Cincinnati, Cincinnati, Ohio

Correspondence
Aleksandr B. Stefaniak, National Institute for Occupational Safety and Health, Morgantown, WV.
Email: AStefaniak@cdc.gov

Abstract

Fused deposition modeling (FDM™) 3-dimensional printing uses polymer filament to build objects. Some polymer filaments are formulated with additives, though it is unknown if they are released during printing. Three commercially available filaments that contained carbon nanotubes (CNTs) were printed with a desktop FDM™ 3-D printer in a chamber while monitoring total particle number concentration and size distribution. Airborne particles were collected on filters and analyzed using electron microscopy. Carbonyl compounds were identified by mass spectrometry. The elemental carbon content of the bulk CNT-containing filaments was 1.5 to 5.2 wt%. CNT-containing filaments released up to 10^{10} ultrafine (d < 100 nm) particles/g printed and 10^{6} to 10^{8} respirable (d ~0.5 to 2 μm) particles/g printed. From microscopy, 1% of the emitted respirable polymer particles contained visible CNTs. Carbonyl emissions were observed above the limit of detection (LOD) but were below the limit of quantitation (LOQ). Modeling indicated that, for all filaments, the average proportional lung deposition of CNT-containing polymer particles was 6.5%, 5.7%, and 7.2% for the head airways, tracheobronchiolar, and pulmonary regions, respectively. If CNT-containing polymer particles are hazardous, it would be prudent to control emissions during use of these filaments.

KEYWORDS

3-D printing, carbon nanotubes, elemental carbon, emission rate, lung deposition modeling, polymer

1 | INTRODUCTION

Additive manufacturing (AM) is a family of processes used to build objects (usually layer-by-layer) from a computer-assisted design program. Material extrusion is one type of AM process and includes fused deposition modeling (FDM™), a technique in which a polymer filament is heated and extruded through a nozzle onto a build plate to create an object. FDM™ has been used in industrial workplaces for over 20 years. More recently, inexpensive "desktop" devices have become available for use in homes, libraries, schools, and small businesses.[1] Though "AM machine" is more technically correct, herein we refer to desktop FDM™ devices using the common term "3-D printer." In 2015, over 275 000 desktop 3-D printers were sold worldwide.[1] Several filament polymers are available for use in desktop 3-D printers, including, but not limited to, acrylonitrile butadiene styrene (ABS), polylactic acid (PLA), and polycarbonate (PC).

Thermal degradation of polymer filaments during 3-D printing has been shown to release millions to billions of ultrafine particles (UFP) per minute and numerous organic chemicals into air.[2-10]

Additives are increasingly being incorporated into polymer filaments to enhance the aesthetic or functional properties of 3-D printed objects. Carbon nanotubes (CNTs) have attracted considerable attention as a polymer additive because of their unique electrical properties.[11,12] However, discrete CNTs and bundles of CNTs are known to induce numerous toxicological and pathological effects in experimental animals and may induce alterations in respiratory and cardiovascular function in workers, though epidemiology studies are not consistent.[13-16] This observed toxicity of native CNTs raises concern about the potential toxicity of inhaling polymer-associated CNT particles.[17] To date, most studies of CNT release from polymer composites have focused on low-energy processes (eg, environmental degradation from UV light) or high-energy processes (eg, drilling and sanding).[18] It is currently unknown whether CNTs are released during thermal degradation of polymer composite filaments used for material extrusion 3-D printing or is there understanding of potential lung deposition if emitted particles are inhaled by workers or members of the general public in schools, libraries, or homes who use or are in proximity to the 3-D printer. Hence, the objectives of this study were to determine whether FDM™ 3-D printing with ABS, PLA, and PC polymer filaments that contain CNTs may present an exposure risk by releasing these engineered nanomaterials into air, as unbound and/or polymer matrix–associated respirable particles, and whether released particles could deposit in the lung.

Practical Implications

- It is known that desktop scale fused deposition modeling 3-dimensional printers emit particles during operation from thermal degradation of feedstock polymer filament; however, the influence of additives on emissions is largely unknown.
- In this study, we demonstrate that 3-dimensional printing with commercially-available acrylonitrile butadiene styrene (ABS), polylactic acid (PLA), and polycarbonate (PC) filaments that contained carbon nanotubes (CNTs) resulted in the release of respirable size polymer particles that contained CNTs.
- It is estimated that 7.2% of these respirable particles could deposit in the alveolar region of the lung.
- If CNT-containing polymer particles are hazardous, it would be prudent to control emissions during use of these filaments in industrial or other environments (homes, etc.) to prevent exposure.

2 | MATERIALS AND METHODS

Three different filaments marketed as containing CNTs were purchased from vendors: ABS filament with multiwalled carbon nanotubes (ABS_{CNT}; 3DXStat ESD, 3DXTech, Byron Center, MI), PLA filament with multiwalled carbon nanotubes (PLA_{CNT}; F-electric Highly Conductive PLA, Functionalize F-Electric, Seattle, WA), and PC filament that contains carbon nanotubes (type considered proprietary) (PC_{CNT}; 3DXStat ESD, 3DXTech). For comparison, ABS and PLA (3DXTech) and PC (Gizmo Dorks LLC, Temple City, CA) filaments of the same polymer type but without CNTs were also evaluated. All filaments were black color to minimize the influence of colorants on particle emissions.[9]

Field emission scanning electron microscopy (FE-SEM, Hitachi S-4800, Tokyo, Japan) was used to analyze surfaces of as-received filament pieces at 5.0 kV accelerating voltage and varying magnifications. Diameters of visible structures consistent with CNTs were measured using ImageJ (freely available for download, see http://rsbweb.nih.gov/ij/download.html), which is supported by the U.S. National Institutes of Health. Additionally, small thin pieces of filaments were placed in 100% EPON™ (epoxy resin in xylene) on a rotator for 3 days, changing the solution every 24 hours. The samples were transferred into flat molds for final embedding. Sections were cut at 70 to 100 nm thickness and imaged using transmission electron microscopy (TEM, JEOL 1400, Tokyo, Japan). Pieces of printed objects were also mounted and analyzed using FE-SEM to determine whether CNTs were present on surfaces.

Organic and elemental carbon (OC and EC) contents of the bulk filaments were measured using thermal-optical analysis. Approximately 4 cm lengths of the composite and base polymer filaments were ground using a SPEX 6870 Freezer/Mill® (SPEX SamplePrep, Metuchen, NJ). Sample vials, containing the filament portion and an impactor (for milling), were loaded into the chamber and precooled in liquid nitrogen for 5 minutes to ensure brittleness. The precooling step was followed by four 2-minute milling sessions, for a total milling period of 8 minutes. After each session, a 2-minute cooling period was used to regain sample brittleness prior to the next cycle. The milling rate was 12 beats/s.

For the OC and EC analyses, small amounts (eg, 150 - 250 μg) of the filament powders were applied to 1.5 cm^2 punches taken from ultraclean quartz-fiber filter media (Pallflex Tissuquartz™, 2500 QAT-UP) and analyzed according to NIOSH Method 5040, based on a thermal-optical technique.[19-21] For analysis of carbon nanomaterials/bulk powders, a manual assignment of the split between OC and EC was made as described in detail previously.[20,22-26] Correction for positive bias in the EC results also was necessary, to account for residual char formed during the analysis due to carbonization of the polymer matrix. For the ABS and PLA materials, the char contribution to the measured EC content of the composites was estimated through analysis of the base polymer filaments (see Results). The OC-EC split was assigned at the beginning of the oxidative mode of the analysis, and the result for the base polymer was subtracted from that for the composite filament. For the PC filaments, extensive carbonization of the polymer matrix precluded a correction by this approach. An estimate of the EC

content of the PC composite was based on the pyrolysis correction feature of the thermal-optical method (Results). In addition to thermal-optical analysis, to determine the oxidation temperature and residual ash (ie, metal impurities), samples were analyzed by thermogravimetric analysis (TGA) using a model Q5000IR analyzer (TA Instruments, Inc.). The instrument was operated under the following conditions: temperature scan from 30 to 850°C, 10°C/min scan rate, balance compartment flow of 10 mL/min (nitrogen), and oven flow of 25 mL/min (air).

2.1 | Chamber setup and air monitoring

Print jobs were performed in a temperature- and humidity-controlled 12.85 m^3 stainless steel chamber which meets international requirements for office equipment emissions testing.[27,28] Air mixing was assessed using sulfur hexafluoride (SF_6) as a tracer gas, and the calculated mixing level (η) was 92% (a level above 80% is considered satisfactory).[27] The leak rate, as assessed using SF_6, was 0.024 air changes per hour, which is negligible compared to the time required for each trial (approximately 0.5 hour for preprinting, 3 to 4 hours for printing (times varied by filament type), and 3 hours postprinting phases). Air entering the chamber was passed through a carbon filter and high-efficiency particulate air (HEPA) filter to remove organic vapors and particles, respectively. The chamber air exchange rate was 1 per hour as determined using SF_6 in a concentration-decay test.[27]

All print jobs were of an artifact from the National Institute of Standards and Technology (NIST)[29] and were printed five times per filament type (except for PLC_{CNT} for which there were only four successful print jobs) using a FDM™ 3-D printer (LulzBot TAZ 5, Aleph Objects, Inc., Loveland, CO). As shown in Figure S1, the test artifact has a 10 × 10 cm base with holes, indentations, and projections. Print settings were as follows (extruder nozzle, °C/print bed, °C): ABS_{CNT} and ABS—240/110; PLA_{CNT}—220/65; PLA—205/60; and PC_{CNT} and PC—290/100. For the PC_{CNT} and PC filaments only, glue (Elmer's Products, Inc., Columbus, OH) was used to adhere objects to the print bed.

2.2 | Particle sampling

Real-time instruments that measure total particle number concentration from 20 nm to 1 μm (P-Trak, Model 8525, TSI Inc., Shoreview, MN), size distribution of particles from 5.6 to 560 nm (fast mobility particle sizer [FMPS], Model 3091, TSI Inc.), and size distribution of particles from 0.5 to 20 μm (aerodynamic particle sizer [APS], Model 3321, TSI Inc.) were used to monitor chamber air before, during, and after printing. The P-Trak and FMPS were used to monitor for the presence of particles smaller than 1 μm which has been the focus for FDM™ printers using base polymer filaments in prior studies.[2-10] The APS was used to evaluate the release of particles with sizes greater than the upper cutoffs of the P-Trak and FMPS during printing. To determine whether the emitted particles were polymer, free CNTs, or CNT/polymer particles, aerosol was collected onto track-etched polycarbonate (TEPC) filters by drawing chamber air through filters at 5 or 10 L/min using a sampling pump (SG10-2, GSA Messgerätebau GmbH, Germany). Separate filter samples were collected before printing (background) and during printing. For each CNT-containing filament, the fraction of emitted particles that contained CNTs was estimated from inspection of the TEPC filter samples collected during printing. We focused the FE-SEM at low magnification near the center of each sample and scanned the filter in either an upward or downward direction in order to decrease the chances of looking at the same location multiple times. When a particle was observed, the magnification was increased and the particle visually examined for any signs of protrusions that resembled a CNT. This protocol was repeated until 75 particles were observed on each filter collected at 5 or 10 L/min for a total of 150 particles per filament type.

2.3 | Carbonyl sampling

All compounds were used as received and had the following purities: O-tert-butylhydroxylamine hydrochloride (TBOX, 99%), O-(2,3,4,5,6-pentafluorobenzyl)hydroxylamine hydrochloride (PFBHA ≥ 98%), toluene (HPLC grade ≥ 99%), glyoxal (40 wt% in water), and methylglyoxal (40 wt% in water) were purchased from Sigma-Aldrich/Fluka (St. Louis, MO). 4-oxopentanal (4-OPA, 98%) was synthesized by Richman Chemical Inc. (Lower Gwynedd, PA) as described previously.[30] Formaldehyde (37% in water) was purchased from Ultra Scientific (N. Kingstown, RI). Methanol (HPLC grade ≥ 99%) was from Fisher Scientific (Pittsburgh, PA). Deionized water (DI H_2O) was distilled, deionized to a resistivity of 18 MΩ-cm, and filtered using a Milli-Q® filter system (Billerica, MA). Helium (UHP grade), the carrier gas, was supplied by Butler Gas (McKees Rocks, PA) and used as received.

Samples were obtained by pulling air from the chamber using a pump (URG 3000-02Q, Chapel Hill, NC) into two 60-mL Teflon® impingers (Savillex, Eden Prairie, MN) containing 25 mL of deionized water at 4.0 L/min per impinger during 3-D printing. Samples were also collected for two air exchanges postrun for comparison. After collection, samples were decanted into 40-mL vials and derivatized with 100 μL aqueous 250 mmol/L TBOX in one vial and 100 μL aqueous 250 mmol/L PFBHA in the other vial. Vials were left overnight to complete derivatization. The next day, 0.5 mL of toluene was added to each vial. The vial was shaken for 30 seconds and allowed to separate into a toluene layer and aqueous layer. For both TBOX- and PFBHA-derivatized samples, 100 μL of the toluene layer was then removed with a pipette and placed in a 2-mL autosampler vial with a 250-μL glass insert (Resetk, Bellefonte, PA). Finally, 1 μL of the extract was analyzed by gas chromatography-mass spectrometry (GC/MS) as described in the Data S1.

2.4 | Calculation of emission rates

Particle emission rates (ER) were calculated separately for each type of real-time instrument (ie, measurement data for the FMPS and APS were not merged into a single data set) using a number-based model

prescribed in the standard RAL-UZ-171 for determination of emissions from office equipment.[31] This model includes a particle loss coefficient to chamber walls in the calculation. The total number of particles emitted during printing was calculated from the ER and print time. The mass of polymer extruded during printing was determined by weighing the printed NIST artifact on a calibrated microbalance (Model XS205, Mettler-Toledo, Greifensee, Switzerland). Finally, yield for each was calculated by dividing the total number of particles emitted during printing by the mass of extruded polymer for each print job.[5]

2.5 | Deposition modeling

The fraction of CNT-containing polymer particles that could deposit in the lung were calculated using the Multiple-Path Particle Dosimetry model (MPPD, v3.04, ARA).[32] Dosimetry estimates were made using the stochastic lung model with 60th percentile size to represent the majority of the general human population. Model parameters were as follows: uniformly expanding flow, upright body position, and oronasal-mouth breather with 0.5 inspiratory fraction and no pause fraction. Breathing parameters were for a Caucasian adult male at light level of activity: Functional residual capacity (3300 mL), upper respiratory tract volume of 50 mL, tidal volume (1000 mL), and breaths per minute (20) are International Commission for Radiological Protection (ICRP) reference human default values.[33] Though the APS measures aerodynamic diameter from <0.523 to 19.8 μm, deposition was only calculated for the ten channels from 0.523 to 1.037 μm (there were very few particle counts above 2 μm) because electron microscopy analysis of emissions (presented in the Results section) indicated that CNTs were mostly associated with polymer particles having sizes of about 0.5 to 1 μm.

2.6 | Statistical analyses

Box plots were created in SigmaPlot (version 13.0, Systat Software, Inc., San Jose, CA). Mean peak number concentration (N_{peak}), ER, yield, and size values were compared between corresponding filament types with or without CNTs (eg, ABS_{CNT} vs ABS) and among CNT-containing filaments using Wilcoxon nonparametric tests. A significance level of $\alpha = 0.05$ was used for all comparisons. Statistics were computed using JMP software (version 12, SAS Institute Inc., Cary, NC).

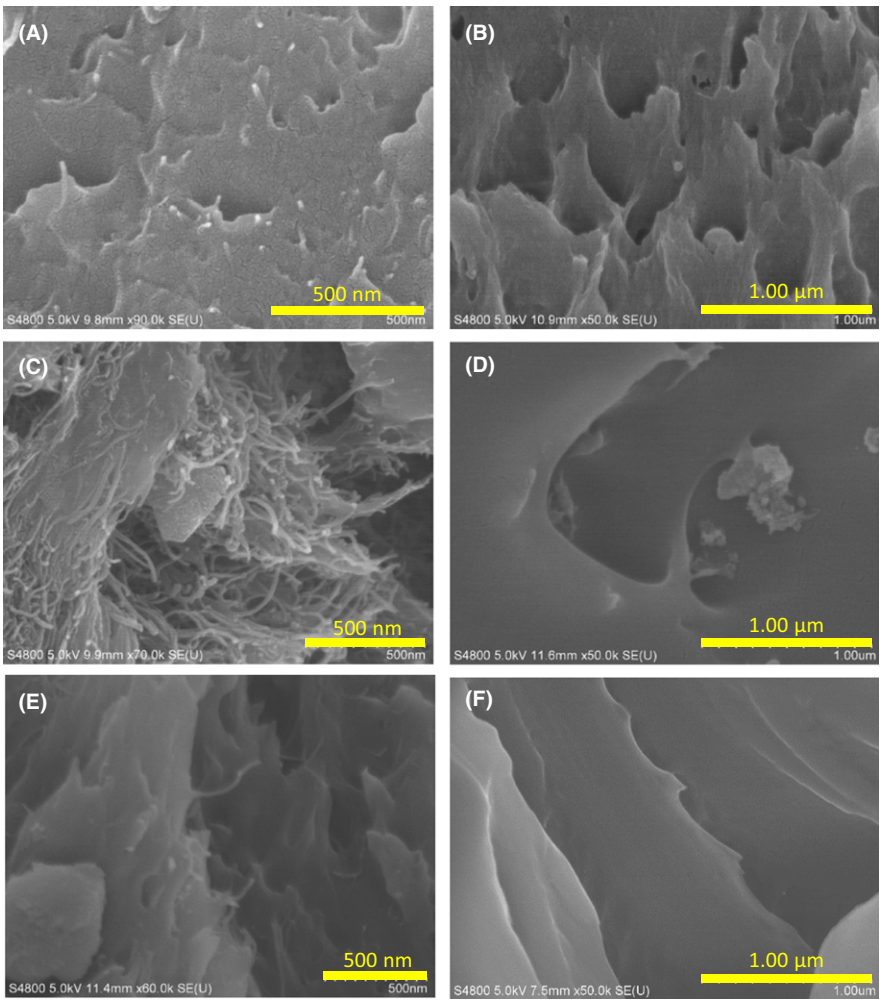

FIGURE 1 Scanning electron micrographs of surfaces of commercially available unused filaments with and without CNTs: (A) ABS_{CNT}, (B) ABS, (C) PLA_{CNT}, (D) PLA, (E) PC_{CNT}, and (F) PC. Note that scale bars differ among images

3 | RESULTS

Figure 1 is FE-SEM images of the surfaces of the as-received bulk filaments. Images of all CNT-containing filaments show smooth areas of polymer with structures consistent with CNTs protruding from the polymer volume onto the surfaces of the filament. Images of the base polymer filaments show smooth areas of filament surfaces with irregular morphology. There was no evidence of CNTs on surfaces of the ABS, PLA, and PC base polymer filaments. TEM analysis of cross-sections of filaments confirmed that CNTs were present in the volume of filaments marketed as CNT-containing filaments but were absent in base polymer filaments (Figure 2). Using ImageJ, the measured average diameters of the CNTs on surfaces of the as-received filaments were 16 ± 3 nm (ABS_{CNT}), 19 ± 4 nm (PLA_{CNT}), and 21 ± 6 nm (PC_{CNT}).

Organic and elemental carbon results for the milled base polymer and composite filaments are reported in Table S1. Details of the results are provided in the Data S1. All materials were fully oxidized during the oxidative mode (920°C maximum) of the analysis (Method 5040). The corrected mean EC content (wt%) of the ABS-CNT composite was about 4% (4.32 ± 0.79%), which was similar to that for the PLA-CNT composite, about 5% (5.20 ± 0.83%). The uncorrected EC contents (wt%) were about 2.2% and 3.7% for the base PC (Gizmo Dorks) and PC_{CNT} (3DX-Tech) filaments, respectively. Because of extensive pyrolysis of the PC matrix, the corrected EC content of the PC composite filament could not be determined through comparison with the base polymer. The (base polymer) corrected EC content of the composite was estimated at about 1.5% (wt%); however, given the high variability of the EC/TC fractions for the PC samples, the accuracy of this result is uncertain.

Details of the results for thermogravimetric analysis are reported in Table S2. The onset of oxidation ranged from 314°C for the PLA materials (polymer and composite) to 474°C for PC_{CNT}. Residual ash contents were relatively low, ranging from 0.06% to about 1%, being highest for PLA_{CNT}.

3.1 | Emission yields and rates

Box plots of yield values by filament type from the real-time particle emission measurements are shown in Figure 3 (examples of number-based concentration measurements from the P-Trak, FMPS, and APS instruments used in the calculations are shown in Figures S2 and S3). In general, yield values calculated from the FMPS data were greater than for the P-Trak data. For particle number measured using

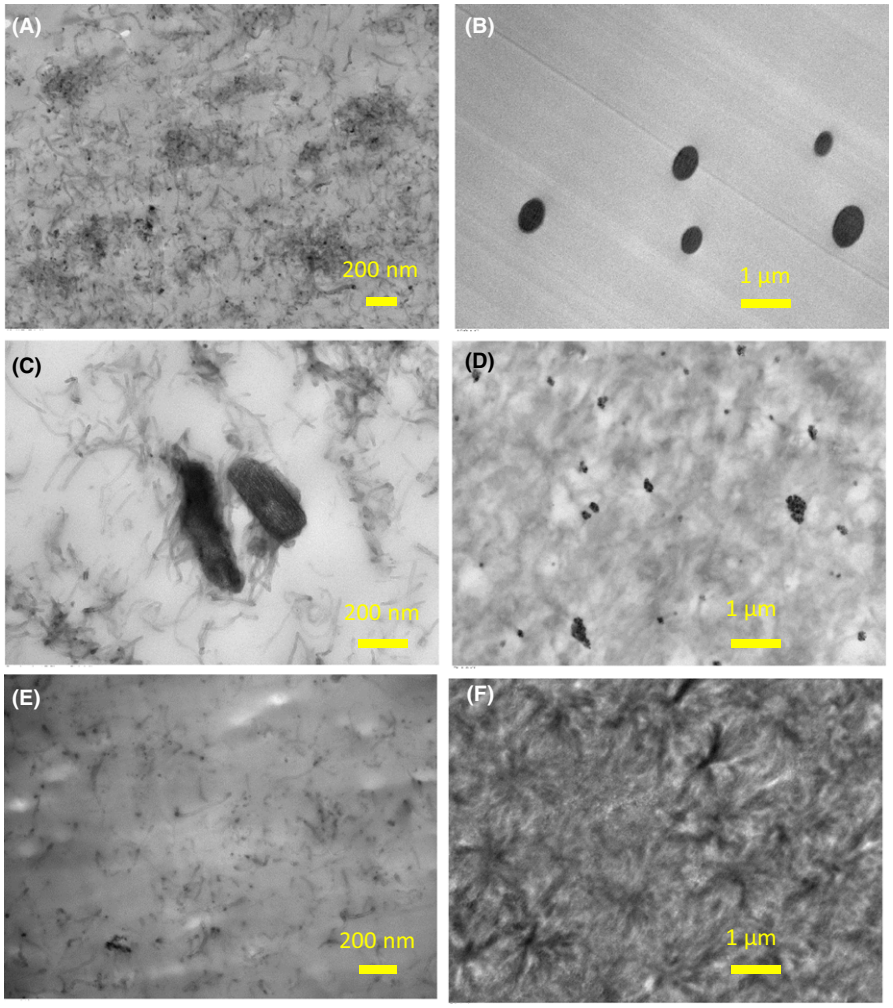

FIGURE 2 Transmission electron micrographs of cross-sections of commercially available filaments labeled for sale with or without CNTs: (A) ABS_{CNT}, (B) ABS, (C) PLA_{CNT}, (D) PLA, (E) PC_{CNT}, and (F) PC. Note that scale bar differs among images

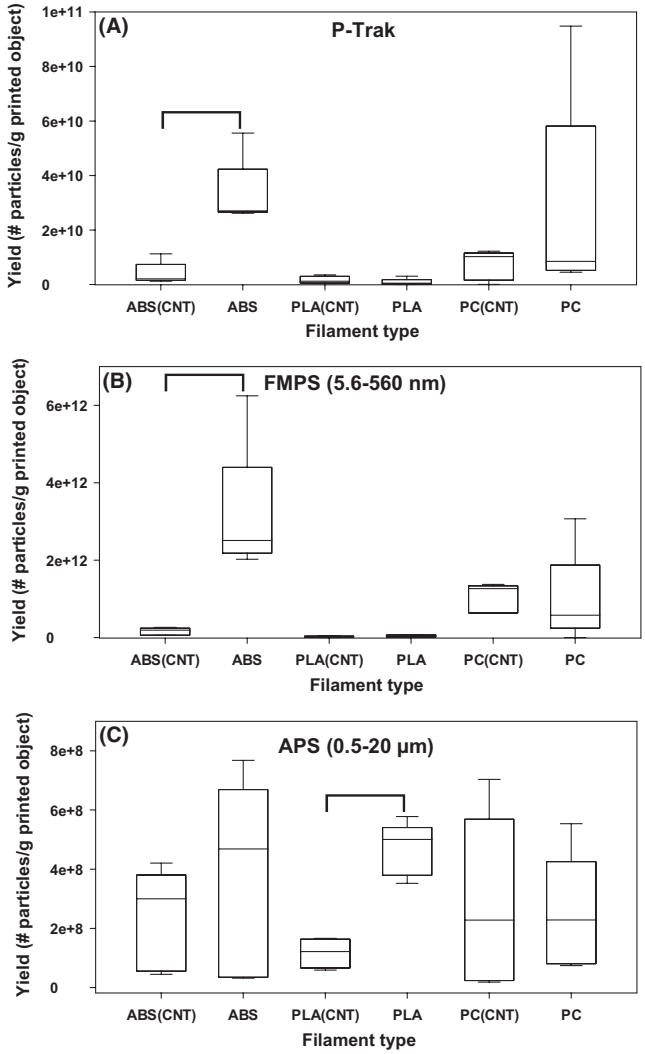

FIGURE 3 Particle emission yields by filament type: (A) number from condensation nuclei counter data (20 nm to 1 µm), (B) number from all FMPS size channels (5.6 to 560 nm), and (C) number from all APS size channels (0.5 to 20 µm). The lower boundary of a box is the 25th percentile, the line within a box is the median, and the upper boundary of a box is the 75th percentile. Whiskers (error bars) below and above a box indicate the 10th and 90th percentiles. Horizontal square bracket = statistical difference ($P < 0.05$). Note the break in the *y*-axis scale in each panel

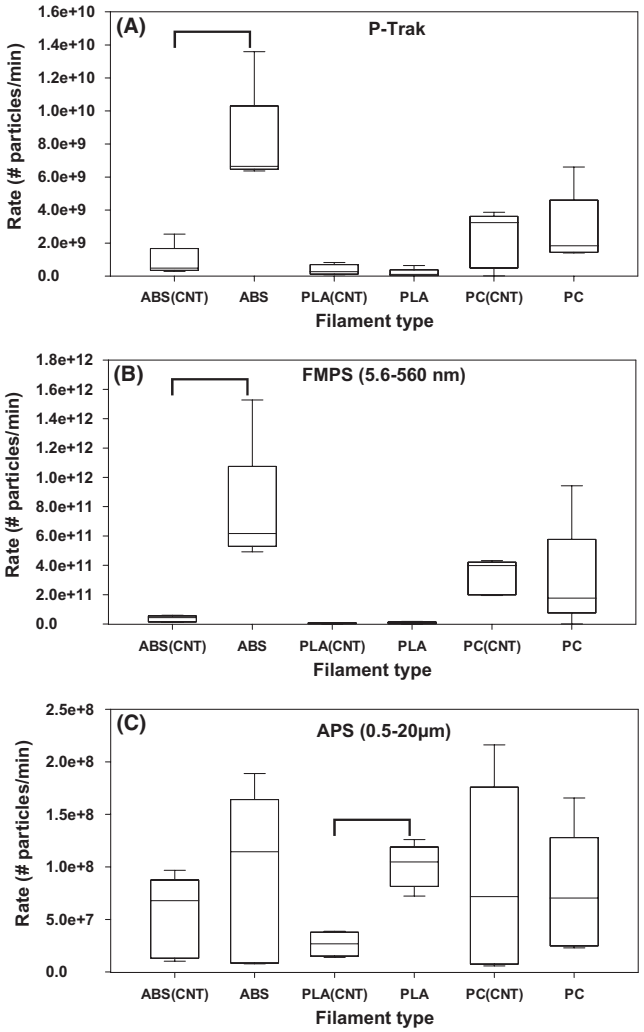

FIGURE 4 Particle emission rates by filament type: (A) number from condensation nuclei counter data (20 nm to 1 µm), (B) number from all FMPS size channels (5.6 to 560 nm), and (C) number from all APS size channels (0.5 to 20 µm). The lower boundary of a box is the 25th percentile, the line within a box is the median, and the upper boundary of a box is the 75th percentile. Whiskers (error bars) below and above a box indicate the 10th and 90th percentiles. Horizontal bracket = statistical difference ($P < 0.05$). Note the break in the *y*-axis scale in each panel

a P-Trak and using a FMPS (all size channels), the yield values for ABS were significantly higher compared to ABS_{CNT}. For particle number measured using the APS (all size channels), the yield value for PLA was significantly higher compared to PLA_{CNT} ($P < 0.05$). Among CNT-containing filaments, yield values determined from particle number measured using a FMPS followed the rank order (from highest to lowest): $PC_{CNT} > ABS_{CNT} > PLA_{CNT}$ ($P < 0.05$); there were no differences among these filaments for measurements made using a P-Trak or APS.

Box plots of calculated ER values for each type of filament are displayed in Figure 4. For particle number measured using a P-Trak and for particle number measured using a FMPS, the ER value for ABS was significantly higher compared to ABS_{CNT}. For particle number measured using an APS, the ER value for PLA was significantly higher compared to PLA_{CNT}. Among CNT-containing filaments, ER values determined from particle number measured using a FMPS followed the rank order (from highest to lowest): $PC_{CNT} > ABS_{CNT} > PLA_{CNT}$ ($P < 0.05$); there were no differences in ER among these filaments for measurements made using a P-Trak or APS.

Box plots of N_{peak} values for each type of filament are shown as Figure 5. N_{peak} values measured using a P-Trak and FMPS differed significantly between PLA_{CNT} and PLA. There were no differences in N_{peak} values among CNT-containing filaments for any instrument used to monitor aerosol in the test chamber.

Individual yield, ER, and N_{peak} values for each print test are given by measurement instrument in Tables S3-S11.

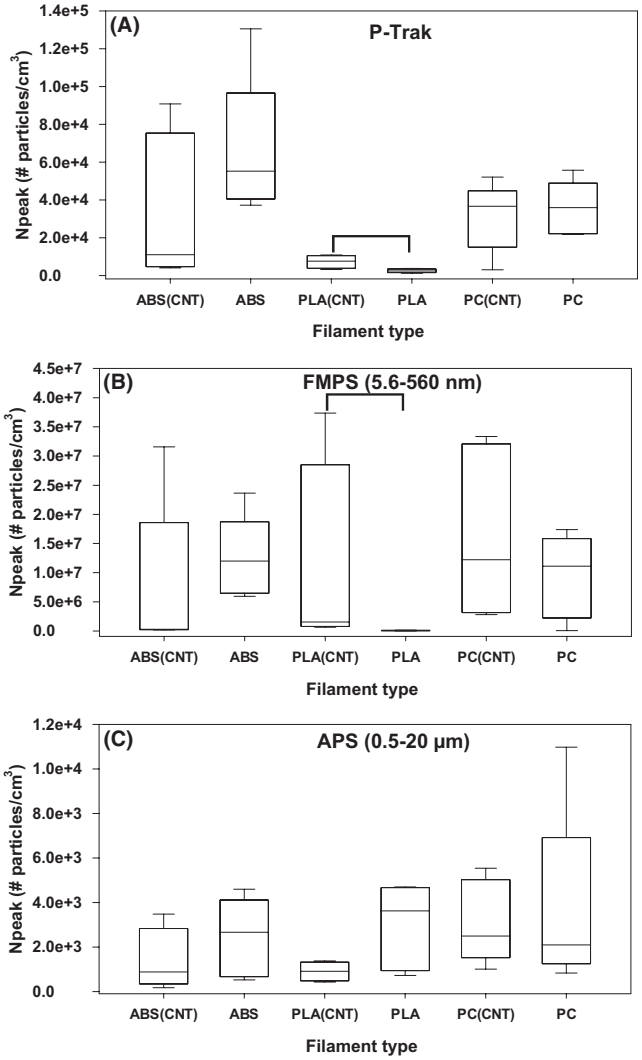

FIGURE 5 Peak particle number concentration (N_{peak}) by filament type: (A) number from condensation nuclei counter data (20 nm to 1 µm), (B) number from all FMPS size channels (5.6 to 560 nm), and (C) number from all APS size channels (0.5 to 20 µm). The lower boundary of a box is the 25th percentile, the line within a box is the median, and the upper boundary of a box is the 75th percentile. Whiskers (error bars) below and above a box indicate the 10th and 90th percentiles. Horizontal bracket = statistical difference ($P < 0.05$). Note the break in the *y*-axis scale in each panel

From the FMPS, average geometric mean (GM) mobility diameters (in nm) and geometric standard deviations (GSD) were 32.8 (1.3), 22.7 (1.3), 21.7 (1.3), 21.6 (1.4), 25.2 (1.3), and 47.5 (1.3) for ABS_{CNT}, ABS, PLA_{CNT}, PLA, PC_{CNT}, and PC, respectively. For each pair of filament types (ABS_{CNT} vs ABS, etc.), mean GM sizes were significantly different ($P < 0.05$). From the APS, average geometric mean (GM) aerodynamic diameters (in nm) and geometric standard deviations (GSD) were 666 (1.2), 661 (1.2), 680 (1.2), 669 (1.2), 653 (1.2), and 675 (1.2) for ABS_{CNT}, ABS, PLA_{CNT}, PLA, PC_{CNT}, and PC, respectively. There were no differences in mean GM size measured using the APS among pairs of filament types. Individual GM and GSD values from the FMPS and APS instruments are given for each type of filament in Tables S12 and S13, respectively.

3.2 | Microscopy of emitted aerosol and printed objects

Figure 6 is scanning electron micrographs of aerosol particles collected during 3-D printing. Printing with CNT-containing filaments released particles having two distinct morphology and size regimes: diffuse clusters of nanoscale polymer particles similar to that seen for the base polymer filaments, and larger solid particles in the submicron to micronscale size range, some of which contained CNTs (Figure 6a, c, and e). For the CNT-containing filaments, no discrete CNTs were observed on the air sample filters nor were CNTs observed associated with the nanoscale cluster particles (data not shown). CNTs were only observed associated with the larger (submicron to micronscale) polymer particles. Printing with base polymer filaments emitted aerosol that was diffuse clusters of nanoscale particles (Figure 6b, d, f). As expected, there was no evidence of CNTs in aerosol emitted while printing with ABS, PLA, or PC base polymer filaments. For the composite filaments, the estimated fraction of emitted particles that contained visible CNTs was 1/150 = 0.7%, 1/150 = 0.7%, and 2/150 = 1.3% for ABS_{CNT}, PLA_{CNT}, and PC_{CNT}, respectively.

Figure 7 is scanning electron micrographs of the surfaces of printed objects. All objects printed using CNT-containing filaments had CNTs visible on the surfaces, whereas objects printed with ABS, PLA, and PC filaments did not.

3.3 | Emission of carbonyl compounds

Carbonyl compounds, which are organic compounds that contain one or more units of a carbon atom double bonded to an oxygen atom, were observed from the 3-D printing emissions. Both mono- and di-carbonyl carbonyl compounds were observed at a level above the limit of detection (LOD) but below the limit of quantitation (LOQ) during the printing and postprinting emissions sampling. Carbonyl concentrations were estimated to be in the subpart per billion (ppb) range (low µg/m^3). The observed carbonyl concentrations were consistently lower during postprint sampling.

3.4 | Particle lung deposition modeling

Table 1 presents the fractional deposition values by region of the respiratory tract calculated using the MPPD software for ABS_{CNT}, PLA_{CNT}, and PC_{CNT} particles for the ten APS size channels from 0.523 to 1.037 µm. These ten channels were used for modeling because electron microscopy analysis of emissions (Figure 6) indicated that CNTs were mostly associated with polymer particles having sizes of about 0.5 to 1 µm. The particle deposition fractions are presented for the head (anterior nasal passages and extrathoracic region or ET_1 and ET_2), bronchiolar (trachea and large bronchi and bronchioles region or BB and bb), and pulmonary (alveolar interstitial or AI) regions.[33] For all filaments, the proportion of CNT-containing polymer particles that could deposit in the respiratory tract for the ten APS size channels from 0.523 to 1.037 µm was 6.51% (range:

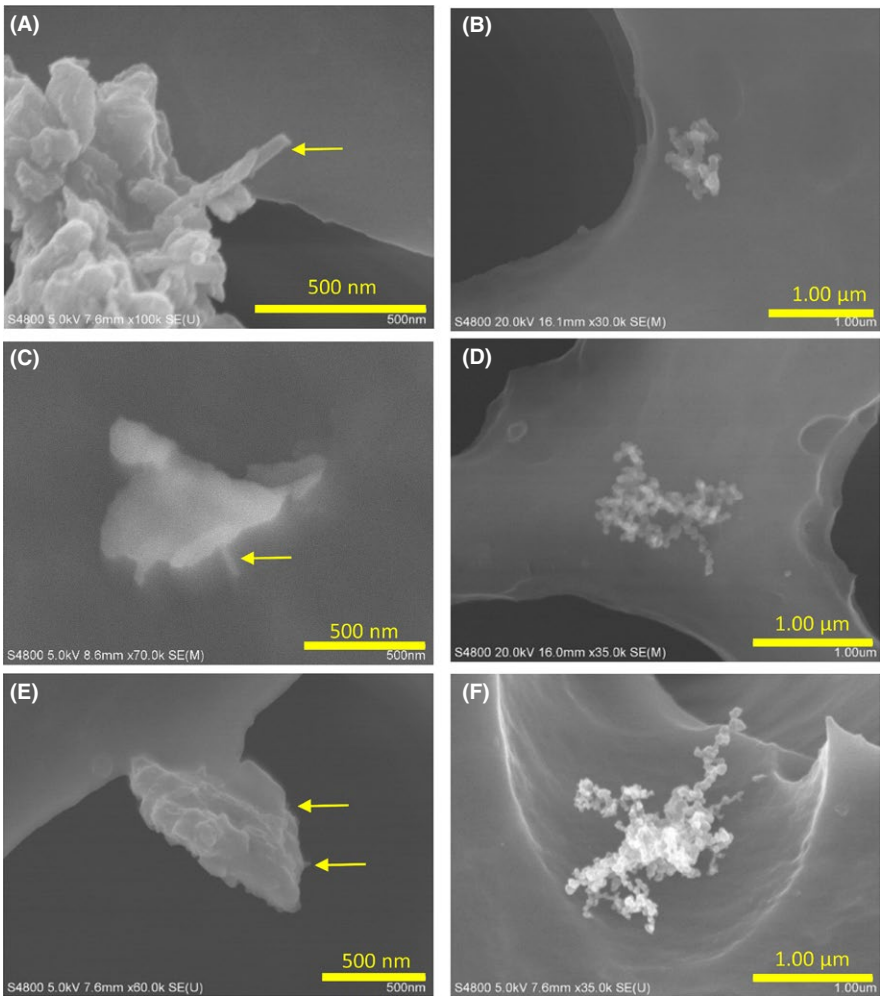

FIGURE 6 Scanning electron micrographs of aerosol particles released during FDM 3-D printing using commercially available filaments with and without CNTs. Printing with nano-enabled filaments released particles that contained CNTs (indicated by arrows), but printing with base polymer filaments did not: (A) ABS_{CNT}, (B) ABS, (C) PLA_{CNT}, (D) PLA, (E) PC_{CNT}, and (F) PC. Note that scale bars differ among images

4.12%-9.96%), 5.74% (range: 5.70%-5.86%), and 7.15% (range: 6.11%-8.92%) for the head, tracheobronchial, and pulmonary regions, respectively.

4 | DISCUSSION

Characterization of the bulk filaments identified the presence of CNTs in all three of the nano-enabled products. Mean diameters of the CNTs were similar regardless of polymer type. The actual CNT content of the filaments is considered proprietary by the manufacturers, though EC content of the bulk filament ranged from 3.7 to 5.2 wt%. NIOSH Method 5040 is based on a thermal-optical analysis technique for OC and EC.[19-21,34] Though this method was developed for monitoring exposure to diesel particulate matter (DPM) as EC,[35] it has general application to carbonaceous aerosols and has been used as a measure of workplace exposure in field studies of CNTs and carbon nanofibers.[20,22-26,36] For thermal-optical analysis of CNT and carbon nanofibers, a manual OC-EC split is assigned rather than the autosplit used with combustion-based aerosols such as DPM. The larger size and agglomerate structure of CNT and carbon nanofibers, together with low air concentrations in workplaces (ie, low filter loadings), make the autosplit unreliable.[20,22-26] Instead, the split is based on results for bulk materials and background samples. Adjustments to the thermal program also may be necessary.[20,22,23,25,37] In this study, environmental background (EC) was not a factor as bulk samples were analyzed, but residual char from carbonization of the polymer matrix posed a positive bias.[25] In the case of PLA and ABS, comparison of the results for the base polymer and corresponding composite filaments allowed estimation of the EC (CNT) content of the composite. However, extensive carbonization of the PC matrix precluded this comparison. An estimate of the CNT content of the PC composite was based on the optical correction feature of the thermal-optical method.

To our knowledge, this is the first report of emissions from use of commercially available CNT-containing 3-D printer filament products. During FDM™ 3-D printing, aerosol particles are formed via thermal degradation of polymer filament in the heated extrusion nozzle and subsequent condensation in air.[10] Particles emitted during printing with base polymer filaments were clusters of spherical nanoscale particles that had a soot-like appearance (Figure 6). Particles emitted during printing with CNT-containing filaments had two distinct morphologies: diffuse clusters of spherical nanoscale particles that had a soot-like appearance (similar to base polymer

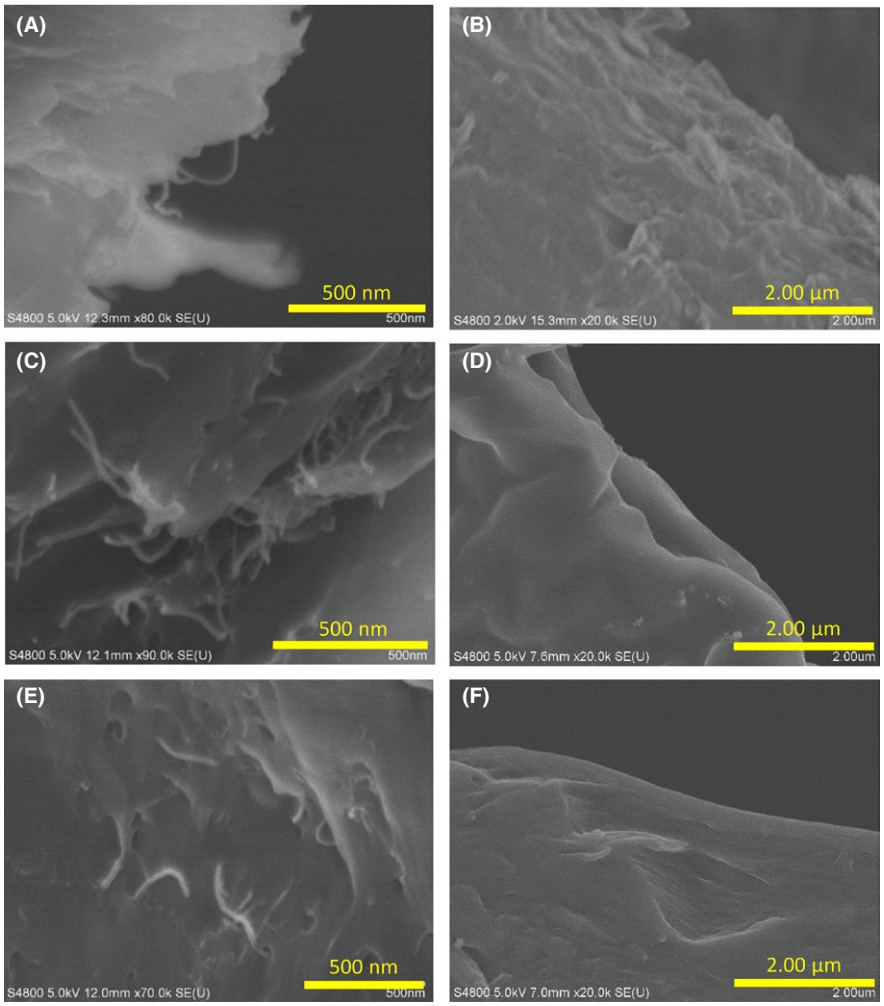

FIGURE 7 Scanning electron micrographs of surfaces of printed objects. Objects printed with nano-enabled filaments had CNTs visible on surfaces, but objects printed with base polymer filaments did not: (A) ABS_{CNT}, (B) ABS, (C) PLA_{CNT}, (D) PLA, (E) PC_{CNT}, and (F) PC. Note that scale bars differ among images

emissions) and solid compact discrete polymer particles in the submicron to micronscale size range, a fraction of which contained CNTs (Figure 6). The soot-like aggregate morphology is from thermal degradation and/or condensation of polymer only. In contrast, the compact submicron to micronscale particle morphology is a combination of polymer and CNTs. This larger compact morphology likely occurs because CNTs that are well dispersed in polymers have high interfacial tension and good compatibility and interface bonding with

TABLE 1 Fractional respiratory tract deposition values for CNT-containing polymer particles

		Fractional deposition		
APS Channel (µm)	Midpoint (µm)	Head	Tracheobronchial	Pulmonary
0.523-0.542	0.533	0.0412	0.0573	0.0611
0.542-0.583	0.563	0.0440	0.0571	0.0619
0.583-0.626	0.605	0.0482	0.0570	0.0632
0.626-0.673	0.650	0.0530	0.0570	0.0651
0.673-0.723	0.698	0.0586	0.0570	0.0676
0.723-0.777	0.750	0.0649	0.0571	0.0706
0.777-0.835	0.806	0.0721	0.0573	0.0742
0.835-0.898	0.867	0.0803	0.0576	0.0785
0.898-0.965	0.932	0.0894	0.0581	0.0835
0.965-1.037	1.001	0.0996	0.0586	0.0892
Average		0.0651	0.0574	0.0715
Range		0.0412-0.0996	0.0570-0.0586	0.0611-0.0892

the matrix, which reduces degradation of the polymer.[38,39] This conclusion is further supported by Figure 2, which demonstrates that CNTs were well dispersed throughout the volumes of the filaments.

Peak number concentrations up to 10^7 particles/cm^3 were observed in chamber testing, indicating all filaments, regardless of additives, emitted a large number of particles during printing. In general, peak number concentrations for ABS and PLA base polymers were consistent with peak concentrations reported in the literature and summarized by Zhang et al.[40] Calculated yield and ER values between pairs of filament types were mostly similar. The exceptions were for ABS, where the yield and ER value for the ABS base polymer were significantly higher compared to ABS_{CNT} (P-Trak and FMPS data), and for PLA, in which the yield and ER values for the base polymer were significantly higher compared to PLA_{CNT} (APS data). Neubauer et al evaluated electrically conductive plastics formed from polyurethane polymer with CNT filler and reported that the release of nanoscale particles during drilling or sanding was lower for plastics with CNTs compared to base polymer.[41] This difference in emission rates between CNT-containing and base polymer filaments may be due to the interfacial tension imparted by the CNTs in the polymer matrix.

The yield and ER values for ABS_{CNT} and PC_{CNT} appeared higher than PLA_{CNT} (Figures 3 and 4), though differences were only significant for values calculated from FMPS data. This observation is interesting because many previous studies of 3-D printing with base polymer filaments have shown that ABS has higher emissions than PLA.[2-5,8-10] Azimi et al evaluated emissions from ABS, PC, and PLA base polymer filaments during 3-D printing, and they determined that emissions for ABS and PC were similar but higher than those for PLA.[2] Similar emission rates among CNT-containing filaments may be due to a common effect of the CNT additive on the polymers.

Calculated emission yields (and rates) were higher for FMPS data relative to P-Trak data. This observation highlights the importance of using multiple complementary instruments to capture emissions across a range of particle sizes. The P-Trak has a purported measurement range of 20 nm to 1 μm, whereas the range of the FMPS is from 5.6 to 560 nm. As shown in Figure S2, particle number concentration values measured by the FMPS for particle sizes from 5.6 to 19.8 nm were orders of magnitude higher than for the P-Trak instrument. This observation indicates that particles with size below 20 nm dominated number-based emissions but could not be measured using the P-Trak. Use of the APS was also important because the sizes of CNT-containing polymer particles were generally in the 0.5 to 2 μm size range which exceeded the upper limit of the FMPS and, for a portion of sizes, also exceeded the upper cutoff of the P-Trak instrument.

As shown in Figure 7, objects printed with CNT-containing filaments had CNTs protruding visibly onto their surfaces. If these objects were further processed by abrasive processes, it could present an inhalation hazard if not performed properly under controlled conditions. For example, it is well known that disturbing composite surfaces by sanding[41-43] or grinding[44] or disrupting the inner volume by drilling or machining[45-47] can generate aerosol that contains CNTs.

The fraction of CNT-containing polymer particles that could deposit in the lung is predicted to range from 6.11% to 8.92% for the pulmonary region. This prediction is important because clearance from the pulmonary region is generally very slow and deposition there would permit prolonged persistence.[33] It is important to recognize that not all deposited particles will remain in the alveoli because the combined effects of chemical and mechanical clearance will remove some fraction. Once deposited, free CNTs that are not cleared are known to be biopersistent in the lung and may induce inflammatory and fibrotic alterations and changes in RNA expression.[48,49] Interestingly, in a life cycle approach, Bishop et al[17] reported that postproduction modification of CNTs by coating them with polymer did not enhance pulmonary injury, inflammation, pathology, or genotoxicity in vitro relative to the as-produced uncoated CNTs and further demonstrated that, for a particular coating, toxicity was significantly attenuated. These authors also collected aerosols generated from sanding composites with embedded polymer-coated CNTs and reported that, similar to our study, some of the released particles were CNT-containing polymer particles (there was no evidence of free CNTs in the aerosol). The polymer-coated CNTs embedded in polymer particles had lower acute in vivo toxicity relative to the as-produced uncoated CNTs.

Carbonyl compounds are of interest because exposure to some chemicals in this class of compounds is associated with respiratory irritation or sensitization in animals.[50-52] While each filament yielded different specific carbonyl emission profiles, no particular filament generated significantly higher carbonyl concentrations than the others. The observed carbonyl emissions concentrations did vary somewhat between print jobs using the same filament, but not significantly. However, based on the observed carbonyl emissions data, printing with these filaments is not expected to significantly contribute to indoor carbonyl concentrations.

5 | CONCLUSIONS

Results from this study demonstrate that FDM™ 3-D printing with CNT-containing filaments emitted CNT-containing polymer particles in the submicron to micronscale size range. No free CNTs were observed in air samples. Modeling indicated the potential for respirable-sized (0.5 to 1 μm) CNT-containing polymer particles to deposit throughout the respiratory tract if emissions are inhaled, though chemical and mechanical clearance mechanisms will remove some fraction. While 3-D printing and nanotechnology are converging to create new possibilities in polymers, our data indicate that material extrusion printing with CNT-containing filaments can release polymer particles that contain CNTs into air. If CNT-containing polymer particles are shown to be hazardous, it would be prudent to control emissions during use of these filaments.

ACKNOWLEDGEMENTS

The authors wish to thank G. Roth and K. L. Dunn at NIOSH for critical review of this manuscript before submission to the journal and J. Fernback for preparation of the EC/OC samples. The findings and conclusions in this report are those of the authors and do not necessarily represent the official position of the National

Institute for Occupational Safety and Health, Centers for Disease Control and Prevention. Mention of any company or product does not constitute endorsement by the National Institute for Occupational Safety and Health, Centers for Disease Control and Prevention.

ORCID

Aleksandr B Stefaniak http://orcid.org/0000-0003-3914-1460

REFERENCES

1. Wohlers. *3D Printing and Additive Manufacturing State of the Industry: Annual Worldwide Progress Report*. Ft. Collins, CO: Wohlers; 2016.
2. Azimi P, Zhao D, Pouzet C, Crain NE, Stephens B. Emissions of ultrafine particles and volatile organic compounds from commercially available desktop three-dimensional printers with multiple filaments. *Environ Sci Technol*. 2016;50(3):1260-1268.
3. Deng Y, Cao SJ, Chen A, Guo Y. The impact of manufacturing parameters on submicron particle emissions from a desktop 3D printer in the perspective of emission reduction. *Build Environ*. 2016;104:311-319.
4. Floyd EL, Wang J, Regens JL. Fume emissions from a low-cost 3-D printer with various filaments. *J Occup Environ Hyg*. 2017;14(7):523-533.
5. Kim Y, Yoon C, Ham S, et al. Emissions of nanoparticles and gaseous material from 3D printer operation. *Environ Sci Technol*. 2015;49(20):12044-12053.
6. Stabile L, Scungio M, Buonanno G, Arpino F, Ficco G. Airborne particle emission of a commercial 3D printer: the effect of filament material and printing temperature. *Indoor Air*. 2017;27(2):398-408.
7. Steinle P. Characterization of emissions from a desktop 3D printer and indoor air measurements in office settings. *J Occup Environ Hyg*. 2016;13:121-132.
8. Stephens B, Azimi P, El Orch Z, Ramos T. Ultrafine particle emissions from desktop 3D printers. *Atmos Environ*. 2013;79:334-339.
9. Yi J, LeBouf RF, Duling MG, et al. Emission of particulate matter from a desktop three-dimensional (3-D) printer. *J Toxicol Environ Health A*. 2016;79:453-465.
10. Vance ME, Pegues V, Van Montfrans S, Leng W, Marr LC. Aerosol emissions from fuse-deposition modeling 3D printers in a chamber and in real indoor environments. *Environ Sci Technol*. 2017;51:9516-9523.
11. Iijima S. Helical microtubules of graphitic carbon. *Nature*. 1991;354(6348):56-58.
12. Dul S, Fambri L, Pegoretti A. Filaments production and fused deposition modelling of ABS/carbon nanotubes composites. *Nanomaterials*. 2018;8(1), http://doi.org/10.3390/nano8010049
13. Dong J, Ma Q. Advances in mechanisms and signaling pathways of carbon nanotube toxicity. *Nanotoxicology*. 2015;9(5):658-676.
14. Beard JD, Erdely A, Dahm MM, et al. Carbon nanotube and nanofiber exposure and sputum and blood biomarkers of early effect among U.S. workers. *Environ Int*. 2018;116:214-228.
15. Kuijpers E, Pronk A, Kleemann R, et al. Cardiovascular effects among workers exposed to multiwalled carbon nanotubes. *Occup Environ Med*. 2018;75(5):351-358.
16. Schubauer-Berigan MK, Dahm MM, Erdely A, et al. Association of pulmonary, cardiovascular, and hematologic metrics with carbon nanotube and nanofiber exposure among U.S. workers: a cross-sectional study. *Part Fibre Toxicol*. 2018;15(1):22.
17. Bishop L, Cena L, Orandle M, et al. In vivo toxicity assessment of occupational components of the carbon nanotube life cycle to provide context to potential health effects. *ACS Nano*. 2017;11(9):8849-8863.
18. Nowack B, David RM, Fissan H, et al. Potential release scenarios for carbon nanotubes used in composites. *Environ Int*. 2013;59:1-11.
19. Birch ME. Analysis of carbonaceous aerosols: interlaboratory comparison. *Analyst*. 1998;123(5):851-857.
20. Birch ME. Monitoring diesel exhaust in the workplace. In: Ashley K, O'Connor PF (eds). *NIOSH Manual of Analytical Methods (NMAM)*, 5th edition. Cincinnati, OH: US Department of Health and Human Services, Centers for Disease Control and Prevention, National Institute for Occupational Safety and Health, DHHS (NIOSH), Publication No. 2014-151; 2016.
21. Birch ME, Cary RA. Elemental carbon-based method for monitoring occupational exposures to particulate diesel exhaust. *Aerosol Sci Technol*. 1996;25(3):221-241.
22. Birch ME, Ku BK, Evans DE, Ruda-Eberenz TA. Exposure and emissions monitoring during carbon nanofiber production–Part I: elemental carbon and iron-soot aerosols. *Ann Occup Hyg*. 2011;55(9):1016-1036.
23. Dahm MM, Schubauer-Berigan MK, Evans DE, Birch ME, Fernback JE, Deddens JA. Carbon nanotube and nanofiber exposure assessments: an analysis of 14 site visits. *Ann Occup Hyg*. 2015;59(6):705-723.
24. Fatkhutdinova LM, Khaliullin TO, Vasil'yeva OL, et al. Fibrosis biomarkers in workers exposed to MWCNTs. *Toxicol Appl Pharmacol*. 2016;299:125-131.
25. NIOSH. *Current Intelligence Bulleting 65: Occupational Exposure to Carbon Nanotubes and Nanofibers*. Cincinnati, OH: National Institute for Occupational Safety and Health; 2013. Report No.: 2013–145.
26. Shvedova AA, Yanamala N, Kisin ER, Khailullin TO, Birch ME, Fatkhutdinova LM. Integrated analysis of dysregulated ncRNA and mRNA expression profiles in humans exposed to carbon nanotubes. *PLoS ONE*. 2016;11(3):e0150628.
27. ASTM. *6670: Standard Practice for Full-Scale Chamber Determination of Volatile Organic Emissions from Indoor Materials/Products*. West Conshohocken, PA: ASTM International; 2013.
28. ISO. *28360: Information technology — Office Equipment — Determination of Chemical Emission Rates from Electronic Equipment*. Geneva, Switzerland: International Organization for Standardization; 2007.
29. Moylan S, Slotwinski J, Cooke A, Jurrens K, Donmez MA. An additive manufacturing test artifact. *J Res Natl Inst Stand Technol*. 2014;119:429-459.
30. Hutton TK, Muir KW, Procter DJ. Switching between novel samarium(II)-mediated cyclizations by a simple change in alcohol cosolvent. *Org Lett*. 2003;5(25):4811-4814.
31. BAM. *Test Method for the Determination of Emissions from Hardcopy Devices*. RAL-UZ-205. St. Augustin, Germany: BAM; 2017.
32. Asgharian B, Hofmann W, Bergmann R. Particle deposition in a multiple-path model of the human lung. *Aerosol Sci Technol*. 2001;34(4):332-339.
33. ICRP (International Commission on Radiological Protection). *Publication 66: Human Respiratory Tract Model for Radiological Protection*, Vol. 24. Oxford, UK: Pergamon; 1994.
34. Birch ME. Occupational monitoring of particulate diesel exhaust by NIOSH method 5040. *Appl Occup Environ Hyg*. 2002;17(6):400-405.
35. NIOSH. Method 5040: Diesel particulate matter (as elemental carbon) (Supplement issued 3/15/2003). In: Ashley K, O'Connor PF, eds. *NIOSH Manual of Analytical Methods*, 4th edn. Cincinnati, OH: US Department of Health and Human Services, Public Health Service, Centers for Disease Control and Prevention, National Institute for Occupational Safety and Health, Publication No. 94-113; 1994.
36. Dahm MM, Evans DE, Schubauer-Berigan MK, Birch ME, Fernback JE. Occupational exposure assessment in carbon nanotube and

nanofiber primary and secondary manufacturers. *Ann Occup Hyg*. 2012;56(5):542-556.
37. Doudrick K, Herckes P, Westerhoff P. Detection of carbon nanotubes in environmental matrices using programmed thermal analysis. *Environ Sci Technol*. 2012;46(22):12246-12253.
38. Gojny FH, Nastalczyk J, Roslaniec Z, Schulte K. Surface modified multi-walled carbon nanotubes in CNT/epoxy-composites. *Chem Phys Lett*. 2003;370(5–6):820-824.
39. Liu S, Wu G, Xiao Y. Multi-interfaces investigation on the PLA composites toughened by modified MWCNTs. *Compos Interface*. 2017;24(8):743-759.
40. Zhang Q, Wong JPS, Davis AY, Black MS, Weber RJ. Characterization of particle emissions from consumer fused deposition modeling 3D printers. *Aerosol Sci Technol*. 2017;51(11):1275-1286.
41. Neubauer N, Wohlleben W, Tomović Ž. Conductive plastics: comparing alternative nanotechnologies by performance and life cycle release probability. *J Nanopart Res*. 2017;19(3):112.
42. Cena LG, Peters TM. Characterization and control of airborne particles emitted during production of epoxy/carbon nanotube nanocomposites. *J Occup Environ Hyg*. 2011;8(2):86-92.
43. Huang G, Park JH, Cena LG, Shelton BL, Peters TM. Evaluation of airborne particle emissions from commercial products containing carbon nanotubes. *J Nanopart Res*. 2012;14(11):1231.
44. Methner M, Crawford C, Geraci C. Evaluation of the potential airborne release of carbon nanofibers during the preparation, grinding, and cutting of epoxy-based nanocomposite material. *J Occup Environ Hyg*. 2012;9(5):308-318.
45. Bello D, Wardle BL, Yamamoto N, et al. Exposure to nanoscale particles and fibers during machining of hybrid advanced composites containing carbon nanotubes. *J Nanopart Res*. 2009;11(1):231-249.
46. Samuel J, DeVor RE, Kapoor SG, Hsia KJ. Experimental investigation of the machinability of polycarbonate reinforced with multiwalled carbon nanotubes. *J Manuf Sci E-T ASME*. 2006;128(2):465-473.
47. Wohlleben W, Meier MW, Vogel S, et al. Elastic CNT-polyurethane nanocomposite: synthesis, performance and assessment of fragments released during use. *Nanoscale*. 2013;5(1):369-380.
48. Snyder-Talkington BN, Dong C, Porter DW, et al. Multiwalled carbon nanotube-induced pulmonary inflammatory and fibrotic responses and genomic changes following aspiration exposure in mice: a 1-year postexposure study. *J Toxicol Environ Health A*. 2016;79(8):352-366.
49. Snyder-Talkington BN, Dong C, Sargent LM, et al. mRNAs and miRNAs in whole blood associated with lung hyperplasia, fibrosis, and bronchiolo-alveolar adenoma and adenocarcinoma after multiwalled carbon nanotube inhalation exposure in mice. *J Appl Toxicol*. 2016;36(1):161-174.
50. Anderson SE, Franko J, Jackson LG, Wells JR, Ham JE, Meade BJ. Irritancy and allergic responses induced by exposure to the indoor air chemical 4-Oxopentanal. *Toxicol Sci*. 2012;127(2):371-381.
51. Anderson SE, Wells J, Fedorowicz A, Butterworth LF, Meade B, Munson AE. Evaluation of the contact and respiratory sensitization potential of volatile organic compounds generated by simulated indoor air chemistry. *Toxicol Sci*. 2007;97(2):355-363.
52. Lima LF, Murta GL, Bandeira AC, Nardeli CR, Lima WG, Bezerra FS. Short-term exposure to formaldehyde promotes oxidative damage and inflammation in the trachea and diaphragm muscle of adult rats. *Ann Anat*. 2015;202:45-51.

SUPPORTING INFORMATION

Additional supporting information may be found online in the Supporting Information section at the end of the article.

How to cite this article: Stefaniak AB, Bowers LN, Knepp AK, et al. Three-dimensional printing with nano-enabled filaments releases polymer particles containing carbon nanotubes into air. *Indoor Air*. 2018;28:840–851. https://doi.org/10.1111/ina.12499